Korean J. Chem. Eng., 40(12), 3096-3105 (2023)
DOI: 10.1007/s11814-023-1577-x

pISSN: 0256-1115
eISSN: 1975-7220

Two-dimensional polymeric cobalt phthalocyanine synthesized by microwave irradiation and its use for continuous glucose monitoring

Sieun Jeon*,‡, Hobin You,‡, Heeyeon An*, and Yongjin Chung*,**,†**

*Department of IT·Energy Convergence, Korea National University of Transportation, 50 Daehak-ro, Chungju, Chungbuk 27469, Korea
**Department of Chemical and Biological Engineering, Korea National University of Transportation, 50 Daehak-ro, Chungju, Chungbuk 27469, Korea
(*Received 16 July 2023 • Revised 4 September 2023 • Accepted 4 October 2023*)

Abstract−Two-dimensional polymeric cobalt phthalocyanine (poly-CoPc) was synthesized using a microwave-assisted process, and its feasibility for use in continuous glucose monitoring (CGM) was investigated. The poly-CoPc/CNT composite showed 18% higher Co content than using commercial CoPc (c-CoPc/CNT) and synthesized CoPc (s-CoPc/CNT) composites, due to its intrinsic polymeric structure. In the cyclic voltammetry test, the bioelectrode incorporating glucose oxidase (GOx) based upper enzyme layer ([poly-CoPc/CNT]/PEI/[GOx-TPA]) demonstrated 1.51 times higher current densities than monomeric CoPc used bioelectrode ([CoPc/CNT]/PEI/[GOx-TPA]). This improvement is attributed to the higher biocompatibility with the enzyme layer of poly-CoPc, which prevents the blocking of hydrophobic sites near the co-factor of GOx. As a glucose sensor, [poly-CoPc/CNT]/PEI/[GOx-TPA] exhibits a sensitivity of 50.5 μA mM^{-1} cm^{-2} and a response time of 2.4 s in the chronoamperometric response test. Furthermore, the proposed bioelectrode showed 95.6% performance maintenance during 24 h and 81.4% stability over 20 days. These findings demonstrate the suitability of [poly-CoPc/CNT]/PEI/[GOx-TPA] for implantable and low-invasive patch-type glucose sensors offering high sensitivity, durability, and a linear response within the physiological glucose concentration range (0.1-20.0 mM) of both average individuals and diabetic patients.

Keywords: Glucose Sensor, Polymeric Cobalt Phthalocyanine, Continuous Glucose Monitoring, Microwave-assisted Synthesis, Glucose Oxidase

INTRODUCTION

Diabetes mellitus is one of the prevalent adult chronic diseases, affecting 10% of the world's population [1]. It is also considered a serious disease, one of the top 10 leading causes of mortality in adults worldwide [2]. However, only half of the patients are able to afford to diagnose and manage their diabetes due to the high cost of diagnostic instruments and the lack of access to these instruments in many parts of the world [3]. Moreover, diabetes must be managed throughout the lifetime through self-monitoring of blood glucose levels since it can cause various geriatric ailments such as kidney and cognitive disorders [4]; many diagnosed patients thus have struggled with a financial burden also. These problems mainly originate from the expensive cost of the glucose-sensing electrodes, which typically consist of precious metal catalysts [5].

Meanwhile, continuous glucose level measurements (CGMs), including low-invasive patch-type or implantable glucose sensors, have attracted public attention recently due to the potential to improve patient comfort and convenience [6]. The widely used medical sensor, the invasive finger-prick test, requires a droplet of blood; the patients thus undergo pain to obtain the diagnostic specimen, commonly collected by sticking a needle on the fingertip. Additionally, the results from this type are less valuable and reliable in monitoring the patient's glucose level than CGMs since the outcome can represent only the value when blood is collected [7-9]. However, the high cost and limited durability of CGM electrodes have hindered their widespread adoption. For instance, a commercially available low-invasive patch-type electrode can be used for only around two weeks, and the expensive electrode thus should be replaced periodically [10,11]. These issues have hindered the accessibility of patients to CGMs, despite the potential benefits. To address these challenges, it is necessary to develop commercially affordable, inexpensive, durable, and sensitive CGM electrodes. Such electrodes would reduce the high social cost of managing diabetes and improve the quality of life for patients with this chronic disease.

So far, various catalysts have been suggested for the glucose level sensor electrode [12-18]. Most of them use glucose oxidase (GOx) enzyme for glucose oxidation reaction (GOR), and Pt electrode serves as the catalyst to generate anodic current from hydrogen peroxide, a product of GOR [19]. Instead of using Pt, in recent years, metal phthalocyanines (MPCs) such as cobalt phthalocyanine (CoPc) have also been considered for use in glucose level sensor electrodes [20-24]. MPCs have shown high sensitivity, specific response to the substrates, chemical stability, and reusability, making them suitable replacements for precious metal-based electrodes [25]. CoPc is one

†To whom correspondence should be addressed.
E-mail: ychung@ut.ac.kr
‡S. Jeon and H. You contributed equally to this work.

of the most widely studied MPCs because of its high catalytic activity toward substrates, high electron transfer capability, and chemically stable nature [26,27]. However, CoPc moieties tend to detach from the support material easily, leading to decreased performance and poor durability. To address this issue, polymeric CoPc has been introduced to form a stable structure through π-conjugated bonding to connect each CoPc moiety in other electrochemical applications such as oxygen reduction reaction [28-30]. However, most of the introduced polymeric-CoPc synthesis methods use complex processes that involve high temperatures [31-33]. This results in higher production costs, which could be a hurdle for commercialization. In conclusion, CoPc is a promising material for use in glucose sensor electrodes. However, further research is needed to develop more efficient and cost-effective methods for synthesizing polymeric CoPc.

In this study, we proposed a microwave (MW)-assisted facile synthesis method for fabricating polymeric CoPc, and its catalytic performances in glucose sensors were demonstrated. So far, CoPc and its derivatives have typically been synthesized using hydrothermal or solvothermal processes. These methods are both time and energy-intensive, significantly contributing to the high manufacturing costs [34]. Moreover, MW-assisted synthesis reduces the amount of solvent required compared to traditional methods. This makes the process more environmentally friendly and economically viable for large-scale production [35]. In our work, we adapted the CoPc synthesis procedure to produce two-dimensional polymeric CoPc. We also optimized the irradiation conditions to enhance its performance as a CGMs catalyst. By adopting the MW synthesis method, fabricated polymeric CoPc showed significantly higher catalytic activity toward hydrogen peroxide oxidation reaction (HPOR), resulting in better selectivity for glucose sensing than monomeric CoPc used catalysts. Furthermore, the prepared bioelectrode also exhibited extended stability and better biocompatibility owing to its structural advantage. In glucose sensing tests, the proposed bioelectrode displayed a linear response in a range of 0.1-20.0 mM, including glucose concentration of human blood and interstitial fluid in healthy bodies and diabetes patients. It indicates that the proposed bioelectrode and polymeric CoPc have enough feasibility to be used for commercial medical sensors in terms of their inexpensive process cost and adequate performance.

To prove the correlation between its unique chemical structure and electrochemical behaviors, various characterizations were applied, including attenuated total internal reflectance Fourier transform infrared (ATR/FTIR), UV-visible spectrometry (UV-Vis), scanning electron microscopy (SEM), and energy-dispersive X-ray spectrometry (EDS), while electrochemical characterization was also employed, including cyclic voltammetry (CV) and Chronoamperometry (CA).

EXPERIMENTAL SECTION

1. Materials

Glucose oxidase (GOx, *Aspergillus Niger*, type X-S, 100,000-250,000 units g^{-1} solid), cobalt(II) phthalocyanine (CoPc, β-form, 97%), 1,2,4,5-tetracyanobenzene (TCNB, 97%), 1,2-dicyanobenzene (DCNB, 98%), poly(ethyleneimine) solution (PEI, ~50% in H_2O), terephtalaldehyde (TPA, 99%), 1,8-diazabicyle[5.4.0]undec-7-ene (DBU, 98%), D-(+)-glucose (≥99.5%), Nafion 117 solution (~5% in a mixture of lower aliphatic alcohols and water), and phosphate buffer solution (pH 7.4, 1.0 M) was purchased from Sigma-Aldrich (USA). Trifluoroacetic acid (TFA, 99%), 1-pentanol (ACS, 99+%), and cobalt(II) chloride (anhydrous, 99.7%, metals basis) were purchased from Alfa Aesar (UK). Multiwall carbon nanotube (CNT) was purchased from Cheaptube (USA). L-ascorbic acid (AA, 99.0%), Uric acid (UA, 98.0%), and Sodium chloride (NaCl, 99.5%) were purchased from Tokyo chemical industry Co., Ltd. (Japan). *N,N*-Dimethylformamide (DMF, 99.0%), dimethyl sulfoxide (DMSO, 99.5%), isopropyl alcohol (IPA, 99.5%), and ethyl alcohol (99.5%) were purchased from Samchun Pure chemical Co., Ltd. (Korea).

2. Synthesis of Catalysts

For synthesizing poly-CoPc, 20 mg of TCNB and 16 mg of cobalt(II) chloride were dissolved in 5 mL of 1-pentanol [36,37]. Afterward, 17.1 μL of DBU was added as a catalyst for the phthalocyanine synthesis reaction, and the mixture was purged with N_2 for 10 minutes. Subsequently, the vial was placed in a MW (Monowave 400, Anton Paar, Austria), and MW was irradiated to the mixture to make the temperature maintain 180 °C for 2 h. After synthesis, any unreacted materials were removed using a centrifuge using ethanol. Once centrifugation was complete, the remaining product was dried in oven at 80 °C for 24 h. For the synthesis of s-CoPc (synthesis-CoPc), the same procedure as the poly-CoPc were applied, except 14.2 mg of DCNB was used instead of TCNB.

For the synthesizing [c-CoPc/CNT] (commercial-CoPc/CNT), 2 mg mL^{-1} of CNT with 1 mM c-CoPc solution (prepared in TFA : DMF=1 : 9) was sonicated for 10 min and stirred gently at room temperature for 2 h. Afterward, the solution centrifuged, and DMF was added to the solid to obtain a solution with a concentration of 5 mg mL^{-1}. The same procedures were followed for fabricating [s-CoPc/CNT] and [poly-CoPc/CNT].

To prepare GOx-TPA, the procedure in previous studies was applied [38,39]. Briefly, a cross-linking agent solution with a concentration of 0.5 mg mL^{-1} was prepared in PBS, and GOx (40 mg mL^{-1}) was added to the solution, followed by a cross-linking reaction at room temperature for 2 h.

3. Fabrication of Electrodes

For half-cell test, glassy carbon electrodes (GCEs) and rotating disk electrodes (RDEs) were used (diameter 5 mm). To fabricate electrodes for H_2O_2 test, 20 μL of catalysts were dropped onto the electrode surface and dried for 2 h. After drying, 10 μL of PEI (2.5 mg mL^{-1} in DIW) was stacked and dried for 1 h. Afterward, a 4 μL of 5wt% Nafion solution was coated on the dried catalyst. This process was repeated to fabricate [c-CoPc/CNT]/PEI, [s-CoPc/CNT]/PEI, and [poly-CoPc/CNT]/PEI electrodes.

For fabricating bioelectrodes for glucose sensing test, 20 μL of aforementioned catalysts were loaded onto GCE, and dried over 2 h. PEI was then stacked, and 10 μL of GOx-TPA enzyme cluster was stacked and dried for 1 h. Finally, a 4 μL of 5 wt% Nafion solution was coated. This process was repeated to fabricate [c-CoPc/CNT]/PEI/[GOx-TPA], [s-CoPc/CNT]/PEI/[GOx-TPA], and [poly-CoPc/CNT]/PEI/[GOx-TPA] electrodes.

4. Characterizations

To examine the electrochemical properties of the catalysts, cyclic

voltammetry (CV) and chronoamperometric response were measured using an SP-240 potentiostat (Bio-logic, USA). A three-electrode system was used, with the prepared electrodes as the working electrode, Ag/AgCl (sat. in 3.0 M NaCl) as the reference electrode, and Pt mesh as the counter electrode. The electrolyte solution was purged with N_2 and air during the measurements. SEM and EDS (JSM-7610F, JEOL, Japan) were employed to examine the surface structure and elemental distribution of the catalysts. UV-Vis spectrometry (NEO-S490, NEOGEN, Korea) and ATR-FTIR (Alpha II, Bruker, germanium crystal) were used to analyze chemical structure.

RESULTS AND DISCUSSION

1. Chemical and Optical Evaluation

ATR/FTIR and UV-Vis spectrometry were performed to evaluate the chemical structure of synthesized CoPcs. Fig. 1(a) presents the ATR/FTIR results of c-CoPc, s-CoPc, and poly-CoPc. Both c-CoPc and s-CoPc exhibited almost the same spectrum, indicating the proposed method is suitable for synthesizing CoPc facilely and eco-friendly. Meanwhile, poly-CoPc showed a different spectrum with significant features of poly-CoPc, as in the previous studies [40-42]. First, the absorption peak of poly-CoPc was broadened, a typical characteristic of the FTIR spectrum of polymers due to the extended molecular structure and intermolecular interaction [43, 44]. The peaks at 1,107 and 1,315 cm^{-1} showed the vibration of the pyrrole ring and C-C stretching in poly-CoPc structure, while the substantial absorption peak at around 1,750 cm^{-1}, which can be assigned unreacted C-N ends [45]. Namely, the ATR/FTIR spectrum of synthesized poly-CoPc exhibited intrinsic features of polymeric CoPc, demonstrating the successful synthesis by MW irradiation.

Fig. 1(b) depicts the UV-Vis spectra of three catalysts dispersed in DMSO. Both CoPcs exhibited two typical absorption peaks, the Q band at 600-700 nm ($a_{1u}\rightarrow e_g(\pi^*)$ transition), and the Soret band (B band) at 300-350 nm ($a_{2u}(\pi)\rightarrow e_g(\pi^*)$ transition), with similar shapes [36,40]. In contrast, poly-CoPc showed the red-shift of the Q band along with an increase in intensity, whereas the B band was blue-shifted and broadened. These features indicate that the synthesized poly-CoPc has a two-dimensional structure [46], which is the expected structure when TCNB is solely used as a

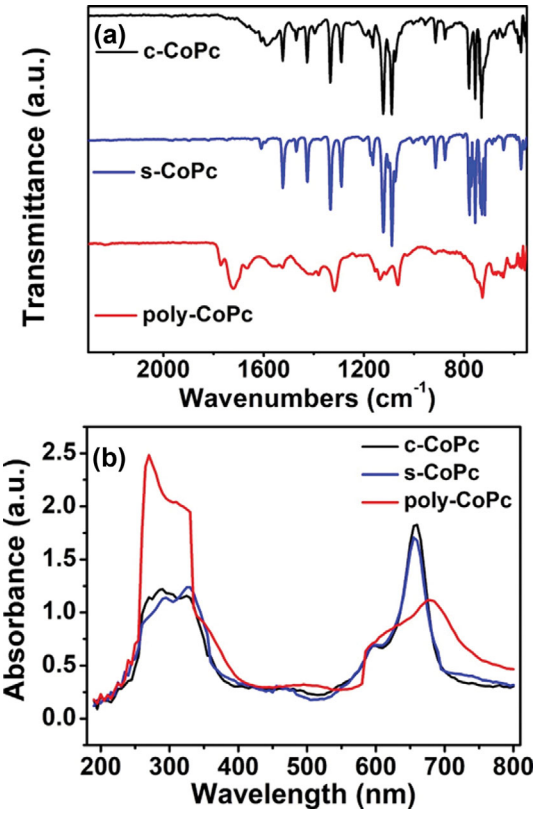

Fig. 1. (a) ATR/FT-IR and (b) UV-Vis spectrum of c-CoPc/CNT, s-CoPc/CNT, and poly-CoPc/CNT.

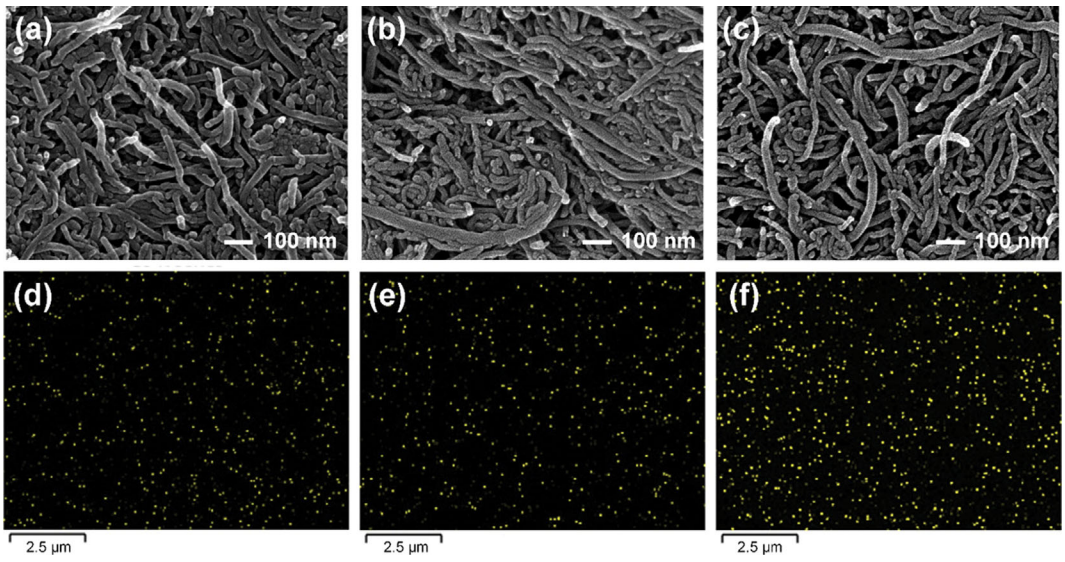

Fig. 2. SEM imiges of (a) c-CoPc/CNT, (b) s-CoPc/CNT, and (c) poly-CoPc/CNT and EDS mapping of Co K series of (d) c-CoPc/CNT, (e) s-CoPc/CNT, and (f) poly-CoPc/CNT.

precursor.

Fig. 2 and Table S1 shows SEM and its Co element EDS mapping images of c-CoPc/CNT, s-CoPc/CNT, and poly-CoPc/CNT composites. In the EDS results, Co elements were well-dispersed onto all around CNT surfaces. However, the Co content in poly-CoPc/CNT (0.59 wt%) was increased compared to monomeric CoPc used composites (0.50 wt%, c-CoPc/CNT and s-CoPc/CNT). This result suggests the use of poly-CoPc contributed to the increase of Co content onto CNT, implying that the polymeric phthalocyanine network structure can prevent the leaching-out of CoPc moieties from the surface of CNT. According to the literature, the high Co content and stronger adhesion of CoPcs lead to better catalytic activity and prolonged catalyst durability, respectively [47-49]. This suggests that poly-CoPc/CNT may have better performance as a HPOR catalyst in bioelectrodes.

In summary, the suggested synthesis method successfully synthesized CoPc and two-dimensional poly-CoPc in an energy-saving and facile way. Additionally, the poly-CoPc contributed to the increase of Co content onto the surface of the CNT supporter, inferring that the poly-CoPc has more robust catalytic activity for HPOR, leading to higher performance of bioelectrode.

2. Electrochemical Measurements.

To evaluate the catalytic activity of poly-CoPc for the HPOR, CV traces of [c-CoPc/CNT]/PEI, [s-CoPc/CNT]/PEI, and [poly-CoPc/CNT]/PEI in H_2O_2 solution were obtained (Figs. 3 and S1). PEI was loaded onto the surface of CoPc/CNTs to enhance electrochemical performance by inducing amine axial ligand coordination with the Co core of CoPc. As shown in Figs. 3(a) and 3(b), anodic currents were observed with an onset potential of around 0.143 V (vs. Ag/AgCl), and increased proportionally to H_2O_2 concentration when [c-CoPc/CNT]/PEI and [s-CoPc/CNT]/PEI were used in the range of 1-5 mM H_2O_2. However, the [poly-CoPc/CNT]/PEI displayed negatively shifted onset potential (0.136 V), and current densities were higher than those of [c-CoPc/CNT]/PEI and [s-CoPc/CNT]/PEI. These results demonstrate that synthesized CoPc has the same catalytic activity as the commercial one, and using poly-CoPc leads to decreased overpotential for HPOR.

Figs. 4 and S2 depict the CV curves of the cascade bioelectrodes for GOR (glucose+O_2+H_2O→H_2O_2+gluconic acid), which consists of the upper GOx enzyme layer and the lower catalyst layer. TPA was used as a cross-liker for GOx to fabricate the enzyme layer to prevent leaching-out from the electrodes and enhance the catalytic activity [38,39,50]. As shown in figures, [poly-CoPc/CNT]/PEI/[GOx-TPA] showed a lower onset potential (0.143 V) than those of [c-CoPc/CNT]/PEI/[GOx-TPA] (0.162 V) and [s-CoPc/CNT]/PEI/[GOx-TPA] (0.165 V) biocatalyst, as expected in Fig. 3. It demonstrates again that the use of poly-CoPc as the catalyst leads to a lower overpotential, which is beneficial for the performance of the bioelectrode.

However, the current densities of [poly-CoPc/CNT]/PEI/[GOx-TPA] steeply increased with glucose concentration more than the others. The current density at 0.45 V of [poly-CoPc/CNT]/PEI/

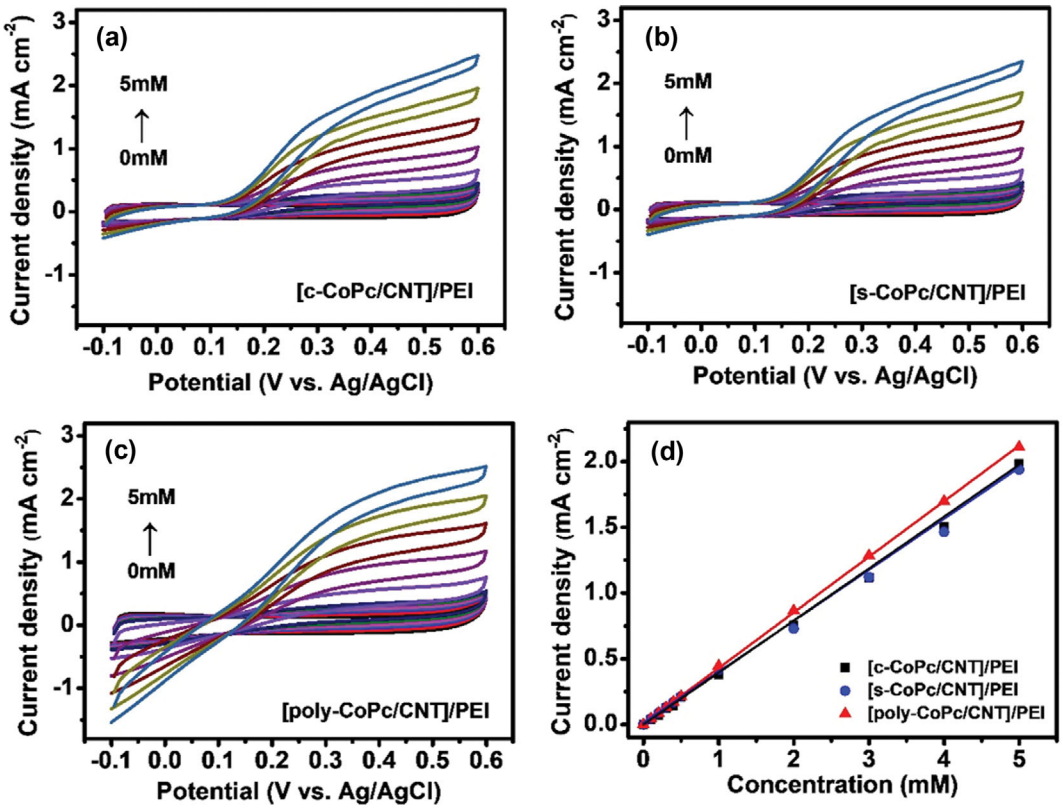

Fig. 3. CV curves of (a) [c-CoPc/CNT]/PEI, (b) [s-CoPc/CNT]/PEI and (c) [poly-CoPc/CNT]/PEI and d) their linear regression results, when 0, 0.1, 0.2, 0.3, 0.4, 0.5, 1, 2, 3, 4, and 5 mM of H_2O_2 were injected. For the tests, 0.1 M PBS (pH 7.4) was used as the electrolyte in N_2 saturated condition, and the potential scan rate was 20 mV s^{-1}.

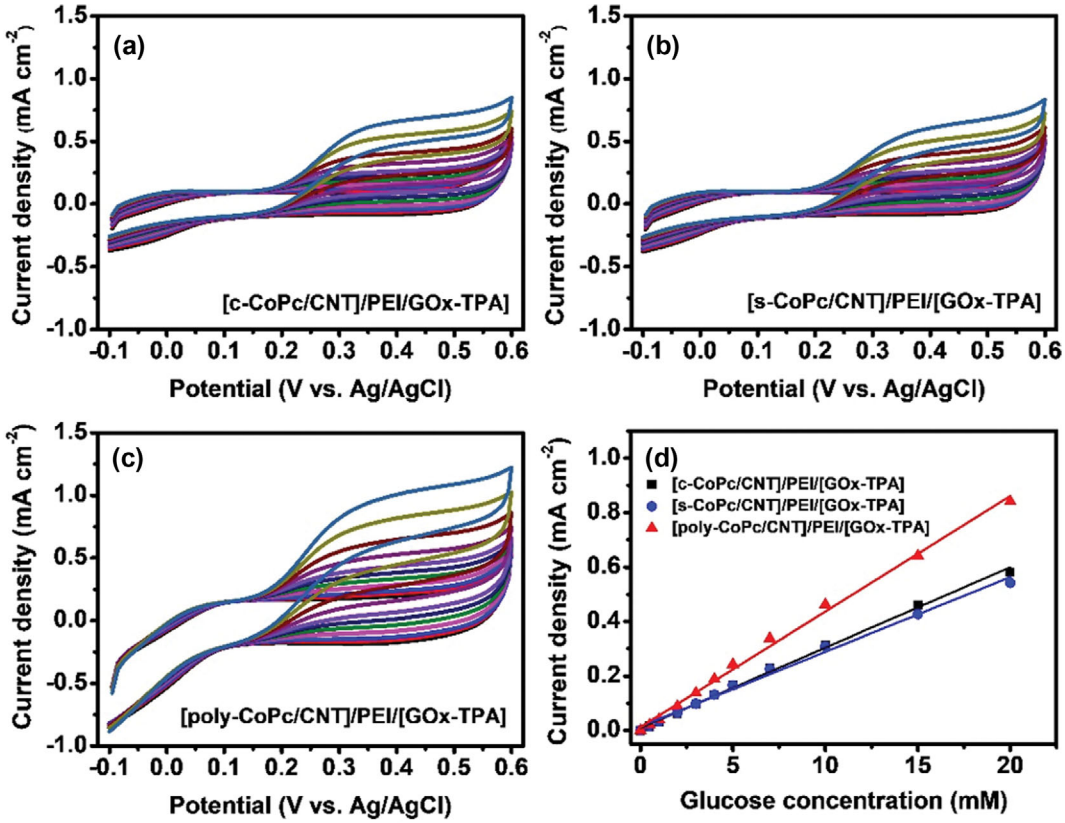

Fig. 4. CV curves of (a) [c-CoPc/CNT]/PEI/[GOx-TPA], (b) [s-CoPc/CNT]/PEI/[GOx-TPA] and (c) [poly-CoPc/CNT]/PEI/[GOx-TPA] and (d) their linear regression results when 0, 0.5, 1, 2, 3, 4, 5, 7, 10, 15 and 20 mM of glucose were injected. For the tests, 0.1 M PBS (pH 7.4) was used as the electrolyte in air saturated condition, and the potential scan rate was 20 mV s^{-1}.

[GOx-TPA] was 0.911 mA cm^{-2}, which is 1.51 times higher than those of [c-CoPc/CNT]/PEI/[GOx-TPA] and [s-CoPc/CNT]/PEI/[GOx-TPA] (around 0.601 mA cm^{-2}), even though the amount of Co is only 18% higher (Fig. 1) and HPOR current destiny is slightly higher (Fig. 3). In other words, the lower [poly-CoPc/CNT]/PEI layer has better biocompatibility with the upper enzyme layer, producing a higher concentration of H_2O_2 in the upper layer. This phenomenon can be explained by the chemical structure of poly-CoPc and the nature of GOx. According to the literature, GOx has a hydrophobic site near FAD (flavin adenine dinucleotide), which is a co-factor of GOx; this site is thus easily connected to or poisoned by hydrophobic materials. As discussed in Fig. 1, the loaded CoPc molecules in [c-CoPc/CNT]/PEI and [s-CoPc/CNT]/PEI can be easily leached out from the surface of CNT, and then the free CoPc can be attached to the hydrophobic site of GOx [51]. These CoPc moieties can block the mass transfer of glucose to FAD or lead to the denaturation of GOx enzymes, resulting in lowering enzyme activity. In contrast, the polymerized CoPc moieties are attached more tightly due to the hydrophobic interaction between the poly-CoPc backbone and CNT structure, causing better biocompatibility with GOx enzyme layer.

Fig. 4(c) demonstrates the linearity of the current densities with glucose concentrations ranging from 0 to 20 mM. As depicted in Fig. 4(c), the current densities of all three catalysts increased proportionally to the glucose concentration within that range. Considering the typical glucose concentration range in human blood of an average individual (4.4-8.3 mM (80-150 mg dL^{-1})) and diabetic patients (hypoglycemia (<4 mM), hyperglycemia (10-20 mM)) [52], the proposed catalytic structures are deemed suitable to use as glucose sensors, and [poly-CoPc/CNT]/PEI/[GOx-TPA] is the best catalyst for sensitivity among three catalysts.

Finally, the rate-determining step (RDS) was determined using the anodic current density values obtained from the cyclic voltammetry (CV) analysis, employing scan rates ranging from 10 to 120 mV s^{-1} after glucose injection (Figs. 5 and S3). The anodic peak current near 0.35 V was used to plot the relationship between the peak current and the scan rate for all electrodes. As a result, the peak current density of all three electrodes increased proportionally to the scan rate, indicating that the two-step reaction is surface-controlled [53].

In summary, [poly-CoPc/CNT]/PEI/[GOx-TPA] exhibits the best sensitivity (42.4 μA mM^{-1} cm^{-2}) compared to catalysts utilizing monomeric CoPc. Additionally, all three catalysts demonstrated linear current density responses with the glucose concentration range of human blood (0.1-20 mM), displaying superior suitability for commercial glucose medical sensor electrodes. These results are attributed to the advantageous characteristics of the poly-CoPc structure and its resulting high biocompatibility with GOx enzyme layer.

The detailed synthesis procedure and the electrode catalytic

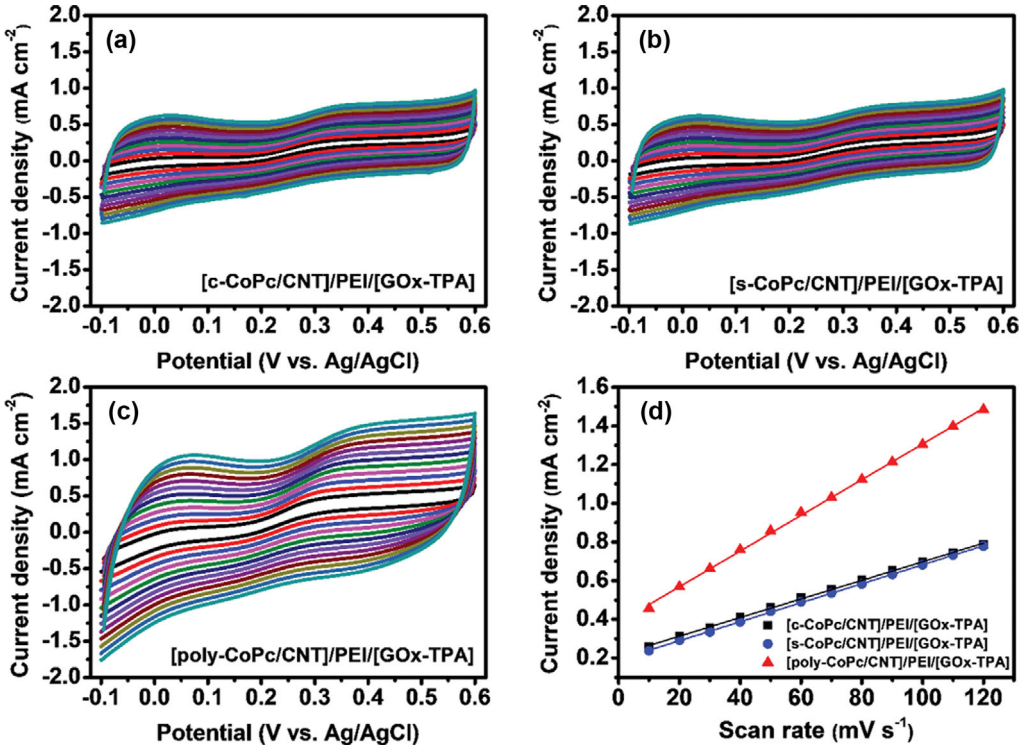

Fig. 5. CV curves of (a) [c-CoPc/CNT]/PEI/[GOx-TPA], (b) [s-CoPc/CNT]/PEI/[GOx-TPA], (c) [poly-CoPc/CNT]/PEI/[GOx-TPA] and (d) their linear regression results based on the current densities measured at 0.35 V at different scan rates (10-120 mV s^{-1}). For the tests, 10 mM glucose in 0.1 M PBS (pH 7.4) was used as the electrolyte in air-saturated condition.

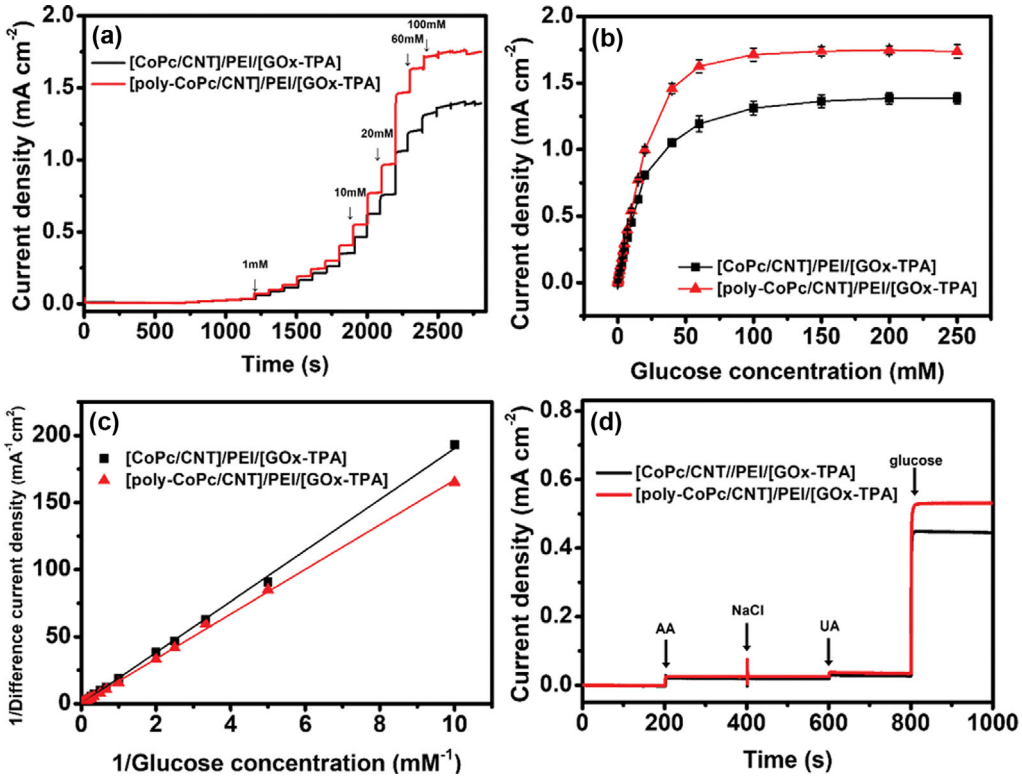

Fig. 6. (a) Chronoamperometric response, (b) plot of glucose concentration against current density, (c) Lineweaver-Berk plot, and (d) interference effect upon the addition of 0.1 mM ascorbic acid (AA), 140 mM NaCl, 0.1 mM uric acid (UA) and 10 mM glucose. For the tests, 0.1 M PBS (pH 7.4) was used as the electrolyte in air-saturated condition, and responses measured at 0.45 V.

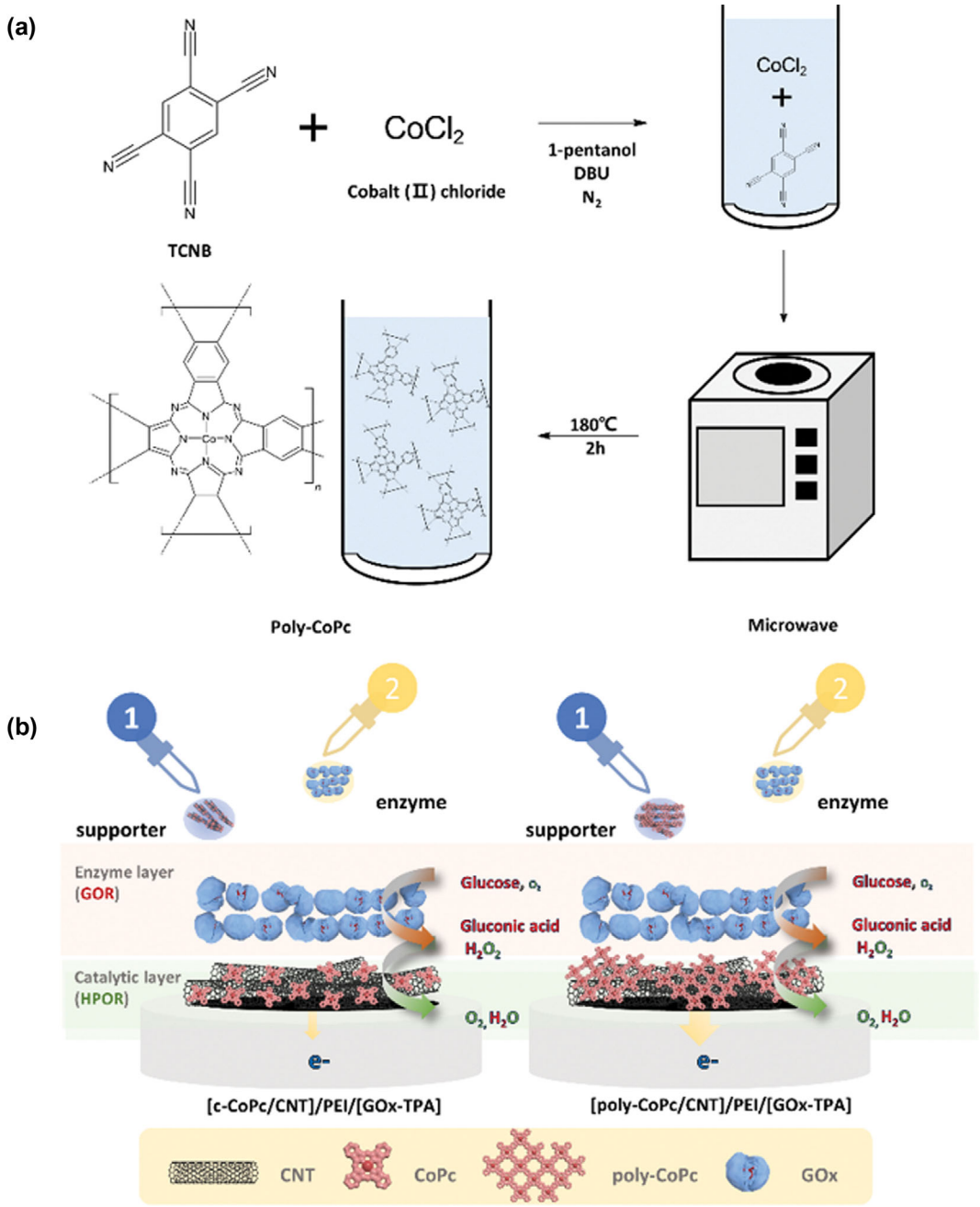

Scheme 1. Schematic illustration of (a) Synthesis mechanism of poly-CoPc and (b) fabrication procedure, reaction mechanism of [c-CoPc/CNT]/PEI/[GOx-TPA] and [poly-CoPc/CNT]/PEI/[GOx-TPA].

structure are illustrated in Scheme 1. Scheme 1(a) represents a MW synthesis process to fabricate poly-CoPc. DBU serves as a catalyst in facilitating the binding of C≡N bonds to form a poly-phthalocyanine structure under the irradiation of MW. Scheme 1(b) illustrates the reaction mechanism of the [c-CoPc/CNT]/PEI/[GOx-TPA] and [poly-CoPc/CNT]/PEI/[GOx-TPA] electrodes. The reaction steps consist of two cascade steps, which are GOR and HPOR. First, glucose is oxidized to gluconic acid and H_2O_2 by GOx on the enzyme layer (Glucose+O_2→Gluconic acid+H_2O_2). The produced H_2O_2 then diffuses to the catalytic layer, CoPc and poly-CoPc catalyzes the decomposition of H_2O_2 via the HPOR (H_2O_2→$2H_2O+2H^++2e^-$) reaction, generating anodic currents.

3. Performance in Amperometric Sensor

To evaluate the feasibility of [poly-CoPc/CNT]/PEI/[GOx-TPA] for use in CGMs and extracorporeal glucose medical sensors, chronoamperometric responses were measured at different glucose concentrations and compared, as shown in Fig. 6(a). For the control sample, [c-CoPc/CNT]/PEI/[GOx-TPA] is used (hereafter denoted as "[CoPc/CNT]/PEI/[GOx-TPA]"). As anticipated, [poly-CoPc/CNT]/PEI/[GOx-TPA] showed steeper linear responses to increasing glucose concentrations compared to those of [CoPc/CNT]/PEI/[GOx-TPA] across the entire measured range (0.1-20.0 mM),

as shown in Fig. 6(b) and S4. The calculated sensitivity to glucose of [poly-CoPc/CNT]/PEI/[GOx-TPA] was 50.5 μA mM^{-1} cm^{-2}, 23.1% enhanced from that of [CoPc/CNT]/PEI/[GOx-TPA] (41.0 μA mM^{-1} cm^{-2}). In terms of response time, that of [poly-CoPc/CNT]/PEI/[GOx-TPA] was calculated to 2.4 s, whereas that of [CoPc/CNT]/PEI/[GOx-TPA] was 4.1 s. This indicates [poly-CoPc/CNT]/PEI/[GOx-TPA] facilitates significantly faster catalytic reaction for GOR-HPOR cascade reaction, leading to more reliable sensing in continuous glucose medical purposes in CGMs. Fig. 6(b) depicts a plot of glucose concentration versus response, obtained by measuring the current densities five times to confirm the excellent reproducibility of the catalyst with negligible deviations.

Fig. 6(c) shows the modified Lineweaver-Burk plot of the catalyst to investigate substrate affinity. The calculated maximum velocity (V_{max}) and Michaelis-Menten constant (K_m) for [poly-CoPc/CNT]/PEI/[GOx-TPA] were determined as 3.60 mA cm^{-2} and 59.9 mM, respectively, while [CoPc/CNT]/PEI/[GOx-TPA] yielded values of 5.25 mA cm^{-2} and 99.8 mM. These results indicate that [CoPc/CNT]/PEI/[GOx-TPA] has a slower reaction rate and lower substrate affinity for glucose substrate compared to [poly-CoPc/CNT]/PEI/[GOx-TPA]. Finally, as shown in Fig. 6(d), the response to common interfering substances, including AA, UA, and NaCl, was investigated. Both catalysts showed minimal responses to interfering substances, highlighting their suitability as glucose sensors from a selectivity perspective.

Shortly, [poly-CoPc/CNT]/PEI/GOx-TPA exhibits superior performance in sensitivity in the range of glucose concentration in human blood compared to [CoPc/CNT]/PEI/[GOx-TPA], attributed to the two-dimensional polymeric characteristic of poly-CoPc, as shown in Table 1. Furthermore, it demonstrates a shorter response time, excellent reproducibility, and selectivity as a glucose medical sensor, demonstrating that it is well-suited for CGMs.

4. Durability and Long-term Stability

Fig. 7(a) presents the result of durability test obtained from the continuous operation of each sensor to evaluate their practical usability in commercial glucose sensors. As observed in the results, two electrodes maintained approximately 95.6% and 88.6% of their initial current densities, respectively. These findings demonstrate that both electrodes can sustain their responses even after 24 h operation. Fig. S6 also supports the high durability of the fabricated

Table 1. Comparison of linear detection range, sensitivity and limit of detection (LOD) for glucose by calculating from CAs

Catalyst	Linear detection range (mM) (R^2)	Sensitivity (μA mM^{-1} cm^{-2})	LOD (mM) (S/N=3)	Ref
[CoPc/CNT]/PEI/[GOx-TPA]	0.1-20 (0.995)	41.0	0.00174	This work
[poly-CoPc/CNT]/PEI/[GOx-TPA]	0.1-20 (0.997)	50.5	0.00136	
GR-CoPc/GOx	0.01-14.8 (0.990)	5.09	0.0016	[54]
RGO/Ag/GOx	0.5-12.5 (0.997)	3.84	0.16	[55]
GOD-NanoCoPc/PGE	0.02-18	7.71	0.005	[21]
Nafion-GOx-SWCNHs modified GCE	0-6	1.06	0.006	[56]
GOD/MCM-41/Nafion/GCE	0.32-15.12 (0.999)		0.18	[57]
Carbon CoPc/GOx ink coated Pt wire	0.35-3.5 (0.998)		0.35	[58]

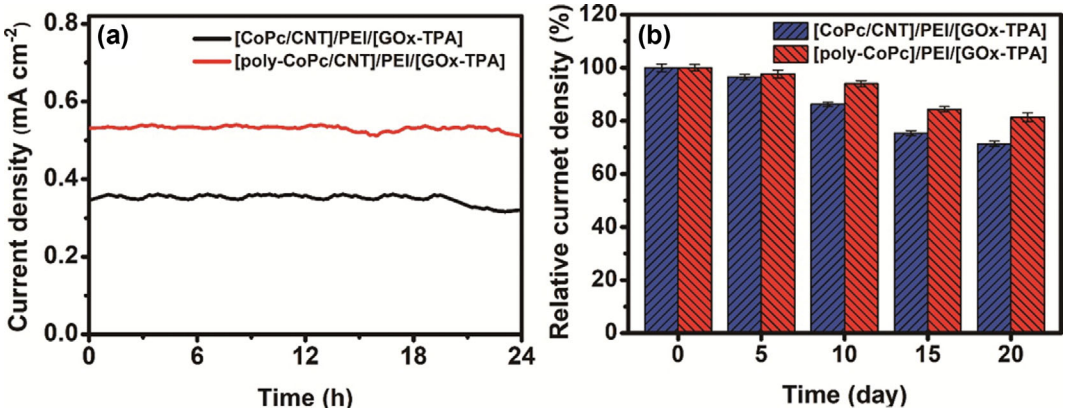

Fig. 7. (a) Durability test result using continuous amperometric response for 24 h and (b) Long-term stability results for 20 days. For the test, 10 mM glucose in 0.1 M PBS (pH 7.4) was used as the electrolyte in air-saturated condition, and responses measured at 0.45 V.

electrode. The two catalysts preserve their CV curve shapes of initial cycle even after 200th cycle CV measurements with or without 10 mM glucose. Fig. 7(b) shows the long-term stability test results measured at 5-day intervals for 20 days. The current measurement responses of [poly-CoPc/CNT]/PEI/[GOx-TPA] and [CoPc/CNT]/PEI/[GOx-TPA] maintained 81.4% and 71.3% of the initial current densities, respectively, indicating the relative stability of the poly-CoPc structure. This enhanced stability can be explained by the effect of the polymeric structure of poly-CoPc. According to several studies, polymeric phthalocyanine-based metallorganic catalysts can maintain their chemical and structural stability better than monomeric phthalocyanine [59-61].

CONCLUSION

Poly-CoPc was synthesized using an MW-assisted process, and its catalytic activity on a bioelectrode for the GOR-HPOR cascade reaction was investigated. Through the proposed synthesis method, the synthesized CoPc (s-CoPc) exhibited a nearly identical chemical structure to the commercially available CoPc (c-CoPc), as confirmed by ATR/FTIR analysis. In contrast, the poly-CoPc displayed a distinctive two-dimensional structural feature in both ATR/FTIR and UV-Vis spectrum. SEM-EDS measurements revealed that the Co content in the fabricated poly-CoPc/CNT composite was approximately 18% higher than that of the s-CoPc/CNT and c-CoPc/CNT composites. This enhancement can be attributed to the polymeric structure of poly-CoPc, which helps prevent the detachment of CoPc moieties from the supporting material through the formation of a polymer network and strong hydrophobic interactions with the surface of CNT.

The catalytic activity towards HPOR was investigated through CV analysis. The current densities of [s-CoPc/CNT]/PEI and [c-CoPc/CNT]/PEI were found to be similar, while [poly-CoPc/CNT]/PEI exhibited slightly higher current densities than [s-CoPc/CNT]/PEI and [c-CoPc/CNT]/PEI with negatively shifted onset potential. These results suggest that poly-CoPc helped reduce the overpotential of HPOR, indicating improved performance for glucose medical sensors. Notably, the effect of poly-CoPc was more pronounced in the bioelectrode. When the prepared bioelectrodes facilitated the two-step (GOR-HPOR) cascade reaction, [poly-CoPc/CNT]/PEI/[GOx-TPA] displayed 1.51 times higher current densities in CV at 0.45 V, showing a linear relationship with the glucose concentration within the range of 0.1-20.0 mM. Taken together, while the catalytic activity towards HPOR was slightly increased, the performance of the bioelectrode for glucose sensing was significantly enhanced. This phenomenon can be attributed to the intrinsic characteristics of the polymeric structure of poly-CoPc, which reduces the blocking effect on the hydrophobic site near the FAD co-factor of GOx caused by CoPc moieties.

The chronoamperometric response tests were conducted to assess the feasibility of [poly-CoPc/CNT]/PEI/[GOx-TPA] for CGMs. The sensitivities of [CoPc/CNT]/PEI/[GOx-TPA] and [poly-CoPc/CNT]/PEI/[GOx-TPA] were recorded as 41.0 and 50.5 $\mu A\ mM^{-1}\ cm^{-2}$ (0.1-20.0 mM), respectively. Additionally, the response time of those were 4.1 and 2.4 s. Furthermore, V_{max} and K_m of [poly-CoPc/CNT]/PEI/[GOx-TPA] were calculated to as 3.60 $mA\ cm^{-2}$ and 59.9 mM, which are clearly enhanced compared to [poly-CoPc/CNT]/PEI/[GOx-TPA]. In terms of durability and long-term stability, the proposed bioelectrode showed 95.6% maintenance of performance for 24 h continuous operation and 81.4% stability over a period of 20 days. These practical results provide evidence that [poly-CoPc/CNT]/PEI/[GOx-TPA] is suitable to use for commercial CGMs, as it exhibits high performances as glucose-sensing electrodes, with a linear response within the concentration range of human blood of an average individual (4.4-8.3 mM (80-150 mg dL^{-1})) and diabetic patients (hypoglycemia (<4 mM), hyperglycemia (10-20 mM)).

ACKNOWLEDGEMENTS

This work was supported by "Regional Innovation Strategy (RIS)" through the National Research Foundation of Korea (NRF) funded by the Ministry of Education (MOE) (2021RIS-001), "Young Researcher Program" through the NRF grant funded by the Ministry of Science and ICT (2020R1C1C1010386), Korea Institute for Advancement of Technology (KIAT) grant funded by the Korea Government (MOTIE) (P0020614, HRD Program for Industrial Innovation), and the Ministry of SMEs and Startups, Republic of Korea (RS202300256612).

SUPPORTING INFORMATION

Additional information as noted in the text. This information is available via the Internet at http://www.springer.com/chemistry/journal/11814.

REFERENCES

1. F. Xiong, J. Wang, J. L. Nierenberg, E. L. Van Blarigan, S. A. Kenfield, J. M. Chan, G. Schmajuk, C.-Y. Huang and R. E. Graff, *Br. J. Cancer.*, **129**, 648 (2023).
2. P. Saeedi, I. Petersohn, P. Salpea, B. Malanda, S. Karuranga, N. Unwin, S. Colagiuri, L. Guariguata, A. A. Motala, K. Ogurtsova, J. E. Shaw, D. Bright and R. Williams, *Diabetes Res. Clin. Pract.*, **157**, 107843 (2019).
3. A. L. Holm, G. S. Andersen, M. E. Jørgensen and F. Diderichsen, *BMJ Open*, **8**, e023211 (2018).
4. K. K. Clemens, N. O'Regan and J. J. Rhee, *Curr. Diab. Rep.*, **19**, 1 (2019).
5. W. Li, W. Luo, M. Li, L. Chen, L. Chen, H. Guan and M. Yu, *Front. Chem.*, **9**, 723186 (2021).
6. L. Johnston, G. Wang, K. Hu, C. Qian and G. Liu, *Front. Bioeng. Biotechnol.*, **9**, 733810 (2021).
7. A. A. Al Hayek, A. A. Robert and M. A. Al Dawish, *Clin. Med. Insights: Endocrinol. Diabetes.*, **12**, 11795514 (2019).
8. L. Olansky and L. Kennedy, *Diabetes Care.*, **33**, 948 (2010).
9. H. Lee, Y. J. Hong, S. Baik, T. Hyeon and D. Kim, *Adv. Healthc Mater.*, **7**, 1701150 (2018).
10. X. Huang, J. Yang, S. Huang, H. jiuan Chen and X. Xie, *Biodes Manuf.*, **5**, 9 (2022).
11. V. Malyško-Ptašinskė, G. Staigvila and V. Novickij, *Front. Bioeng. Biotechnol.*, **10**, 1094968 (2023).

12. S. Jeon, J. Ji, H. An, Y. Kwon and Y. Chung, *Mater. Chem. Phys.*, **267**, 124615 (2021).
13. V. B. Juska and M. E. Pemble, *Sensors*, **20**, 6013 (2020).
14. B. C. Kang, B. S. Park and T. J. Ha, *Appl. Surf. Sci.*, **470**, 13 (2019).
15. H. An, H. Jeon, J. Ji, Y. Kwon and Y. Chung, *J. Energy Chem.*, **58**, 463 (2021).
16. B. B. Kamble, P. Talele, A. K. Tawade, K. K. Sharma, S. S. Mali, C. K. Hong and S. N. Tayade, *Korean J. Chem. Eng.*, **39**, 1604 (2022).
17. J. Lee, K. Hyun and Y. Kwon, *Korean J. Chem. Eng.*, **40**, 1775 (2023).
18. T. V. Dang and M. I. Kim, *Korean J. Chem. Eng.*, **40**, 302 (2023).
19. X. Wang, J. H. Kim, Y. B. Choi, H. H. Kim and C. J. Kim, *Korean J. Chem. Eng.*, **36**, 1172 (2019).
20. H. Wang, Y. Bu, W. Dai, K. Li, H. Wang and X. Zuo, *Sens. Actuators B Chem.*, **216**, 298 (2015).
21. K. Wang, J. J. Xu and H. Y. Chen, *Biosens. Bioelectron.*, **20**, 1388 (2005).
22. F. Haghighian, S. M. Ghoreishi, A. Attaran, F. Z. Kashani and A. Khoobi, *Korean J. Chem. Eng.*, **40**, 650 (2023).
23. S. Jeon, H. An and Y. Chung, *Sustain. Energy Fuels.*, **6**, 841 (2022).
24. J. Ji, K. Im, H. An, S. J. Yoo, Y. Chung, J. Kim and Y. Kwon, *Int. J. Energy Res.*, **46**, 760 (2022).
25. R. R. Cranston and B. H. Lessard, *RSC Adv.*, **11**, 21716 (2021).
26. T. Kondo, M. Horitani and M. Yuasa, *Int. J. Electrochem.*, **2012**, 6 (2012).
27. K. I. Ozoemena and T. Nyokong, *Electrochim. Acta*, **51**, 5131 (2006).
28. H. Wu, Y. Cao, G. Zhu, D. Zeng, X. Zhu, J. Du and L. He, *Chem. Commun.*, **56**, 3637 (2020).
29. N. B. McKeown, *J. Mater. Chem.*, **10**, 1979 (2000).
30. H. An, C. Noh, S. Jeon, Y. Kwon and Y. Chung, *J. Energy Storage.*, **68**, 107796 (2023).
31. P. M. Budd, S. M. Makhseed, B. S. Ghanem, K. J. Msayib, C. E. Tattershall and N. B. McKeown, *Mater Today.,* **7**, 40 (2004).
32. K. P. C. P., K. Rayappa Naveen, S. Aralekallu, Shivalingayya and L. Koodlur Sannegowda, *RSC Sustain.*, **1**, 128 (2023).
33. M. Wang, S. Fu, P. Petkov, Y. Fu, Z. Zhang, Y. Liu, J. Ma, G. Chen, S. M. Gali, L. Gao, Y. Lu, S. Paasch, H. Zhong, H. P. Steinrück, E. Cánovas, E. Brunner, D. Beljonne, M. Bonn, H. I. Wang, R. Dong and X. Feng, *Nat. Mater*, **22**, 880 (2023).
34. P. T. Phan, J. Hong, N. Tran and T. H. Le, *Nanomaterials*, **13,** 352 (2023).
35. N. Han, Y. Wang, L. Ma, J. Wen, J. Li, H. Zheng, K. Nie, X. Wang, F. Zhao, Y. Li, J. Fan, J. Zhong, T. Wu, D. J. Miller, J. Lu, S. T. Lee and Y. Li, *Chem. Soc. Rev.*, **3**, 652 (2017).
36. N. Han, Y. Wang, L. Ma, J. Wen, J. Li, H. Zheng, K. Nie, X. Wang, F. Zhao, Y. Li, J. Fan, J. Zhong, T. Wu, D. J. Miller, J. Lu, S. T. Lee and Y. Li, *Chem. Soc. Rev.*, **3**, 652 (2017).
37. Y. Tanamura, T. Uchida, N. Teramae, M. Kikuchi, K. Kusaba and Y. Onodera, *Nano Lett.*, **1**, 387 (2001).
38. Y. Chung, K. H. Hyun and Y. Kwon, *Nanoscale*, **8**, 1161 (2015).
39. Y. Chung, D. C. Tannia and Y. Kwon, *Chem. Eng. J.*, **334**, 1085 (2018).
40. J. Chen, K. Zou, P. Ding, J. Deng, C. Zha, Y. Hu, X. Zhao, J. Wu, J. Fan, Y. Li, J. M. Chen, K. Y. Zou, P. Ding, J. Deng, C. Y. Zha, Y. P. Hu, X. Zhao, J. L. Wu, J. Fan and Y. G. Li, *Adv. Mater.*, **31**, 1805484 (2019).
41. S. Wei, H. Zou, W. Rong, F. Zhang, Y. Ji and L. Le Duan, *Appl. Catal. B.*, **284**, 119739 (2021).
42. V. I. Korepanov and D. M. Sedlovets, *Mater. Res. Express.*, **6**, 5 (2019).
43. M. M. Coleman, A. M. Lichkus and P. C. Painter, *Macromolecules*, **22**, 586 (1989).
44. C. Lau, S. Zheng, Z. Zhong and Y. Mi, *Macromolecules*, **31**, 7291 (1998).
45. D. Wöhrle and E. Preußner, *Makromol. Chem.*, **186**, 2189 (1985).
46. B. Ortiz, S. Park and N. Doddapaneni, *Mater. Res. Express.*, **143**, 1800 (1996).
47. S. Jeon, H. An, J. Ji, Y. Kwon and Y. Chung, *Int. J. Energy Res.*, **46**, 4142 (2022).
48. J. Ji, C. Noh, Y. Chung and Y. Kwon, *J. Mater. Chem. C.*, **9**, 14675 (2021).
49. S. Jeon, H. An, C. Noh, Y. Kwon and Y. Chung, *Appl. Surf. Sci.*, **613**, 155962 (2023).
50. Y. Chung, Y. Ahn, M. Christwardana, H. Kim and Y. Kwon, *Nanoscale*, **8**, 9201 (2016).
51. M. Christwardana, Y. Chung and Y. Kwon, *NPG Asia Mater.*, **9**, e386 (2017).
52. P. E. Cryer, S. N. Davis and H. Shamoon, *Diabetes Care.*, **26**, 1902 (2003).
53. H. An, C. Noh, S. Jeon, M. Shin, Y. Kwon and Y. Chung, *Int. J. Energy Res.*, **46**, 11802 (2022).
54. V. Mani, R. Devasenathipathy, S. M. Chen, S. T. Huang and V. S. Vasantha, *Enzyme Microb. Technol.*, **66**, 60 (2014).
55. S. Palanisamy, C. Karuppiah and S. M. Chen, *Colloids Surf. B.*, **114**, 164 (2014).
56. J. D. Qiu, W. M. Zhou, J. Guo, R. Wang and R. P. Liang, *Anal. Biochem.*, **385**, 264 (2009).
57. Z. H. Dai, J. Ni, X. H. Huang, G. F. Lu and J. C. Bao, *Bioelectrochemistry*, **70**, 250 (2007).
58. R. M. Pemberton, T. Cox, R. Tuffin, I. Sage, G. A. Drago, N. Biddle, J. Griffiths, R. Pittson, G. Johnson, J. Xu, S. K. Jackson, G. Kenna, R. Luxton and J. P. Hart, *Biosens. Bioelectron.*, **42**, 668 (2013).
59. S. Yang, Y. Yu, X. Gao, Z. Zhang and F. Wang, *Chem. Soc. Rev.*, **50**, 12985 (2021).
60. S. De, T. Devic and A. Fateeva, *Dalton Trans.*, **50**, 1166 (2021).
61. A. Singh, S. Roy, C. Das, D. Samanta and T. K. Maji, *Chem. Commun.*, **54**, 4465 (2018).

Supporting Information

Two-dimensional polymeric cobalt phthalocyanine synthesized by microwave irradiation and its use for continuous glucose monitoring

Sieun Jeon[*,‡], Hobin You[,‡], Heeyeon An[*], and Yongjin Chung[*,**,†]**

*Department of IT·Energy Convergence, Korea National University of Transportation, 50 Daehak-ro, Chungju, Chungbuk 27469, Korea
**Department of Chemical and Biological Engineering, Korea National University of Transportation, 50 Daehak-ro, Chungju, Chungbuk 27469, Korea
(*Received 16 July 2023 • Revised 4 September 2023 • Accepted 4 October 2023*)

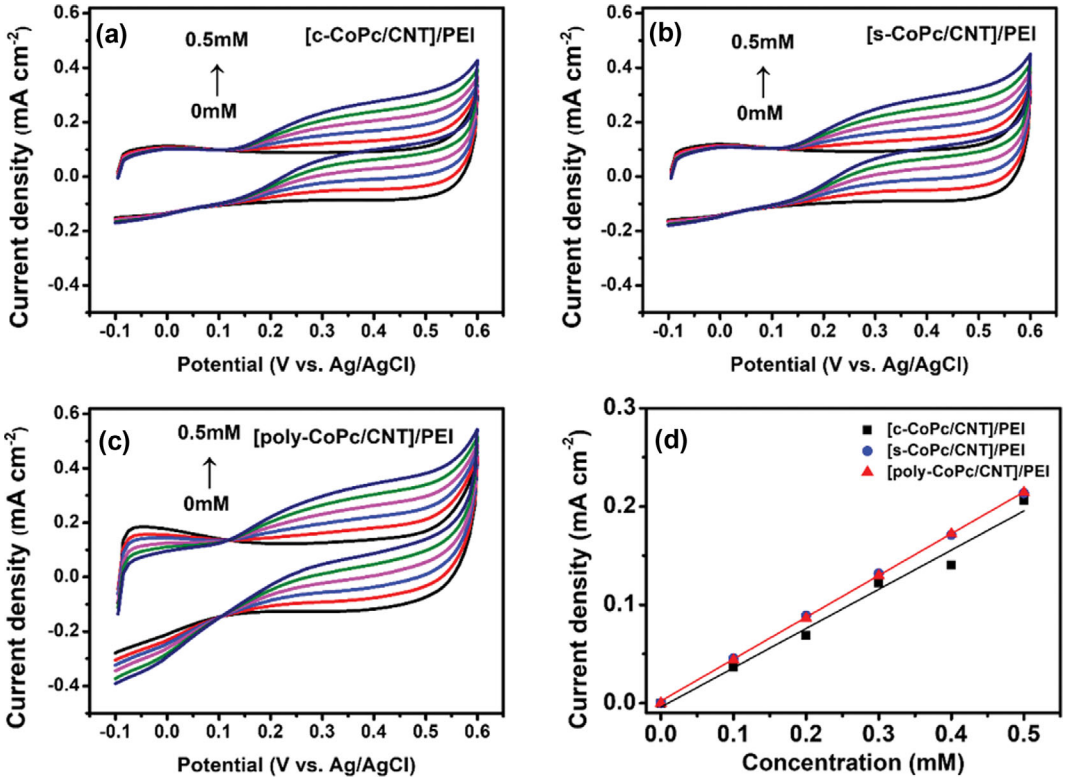

Fig. S1. CV curves of (a) [c-CoPc/CNT]/PEI, (b) [s-CoPc/CNT]/PEI, (c) [poly-CoPc/CNT]/PEI and (d) their linear regression results based on the current densities measured at 0.45 V when 0, 0.1, 0.2, 0.3, 0.4 and 0.5 mM of H_2O_2 were injected. For the tests, 0.1 M PBS (pH 7.4) was used as the electrolyte in N_2 saturated condition, and the potential scan rate was 20 mV s^{-1}.

Table S1. Weight percentages of Co in catalysts measured by SEM-EDS

Sample	Element mass fraction (wt%)			
	1	2	3	Average
c-CoPc/CNT	0.47	0.49	0.54	0.50±0.021
s-CoPc/CNT	0.50	0.53	0.47	0.50±0.017
poly-CoPc/CNT	0.62	0.57	0.58	0.59±0.015

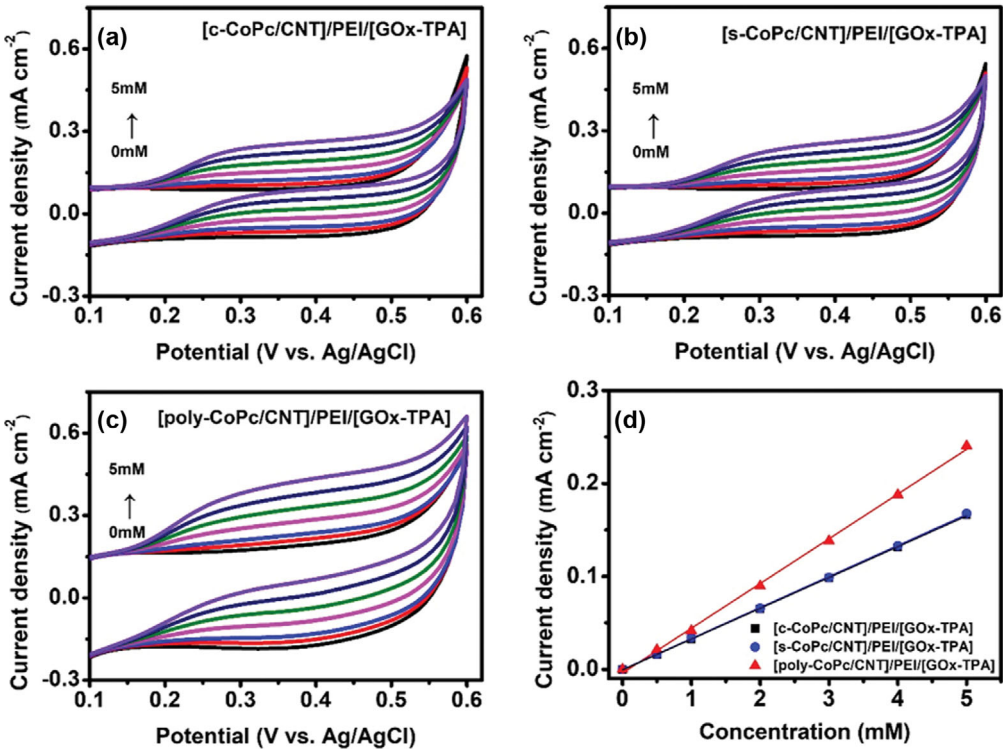

Fig. S2. CV curves of (a) [c-CoPc/CNT]/PEI/[GOx-TPA], (b) [s-CoPc/CNT]/PEI/[GOx-TPA], (c) [poly-CoPc/CNT]/PEI/[GOx-TPA] and (d) their linear regression results based on the current densities measured at 0.45 V when 0, 0.5, 1, 2, 3, 4 and 5 mM of glucose were injected. For the tests, 0.1 M PBS (pH 7.4) was used as the electrolyte in air saturated condition, and the potential scan rate was 20 mV s^{-1}.

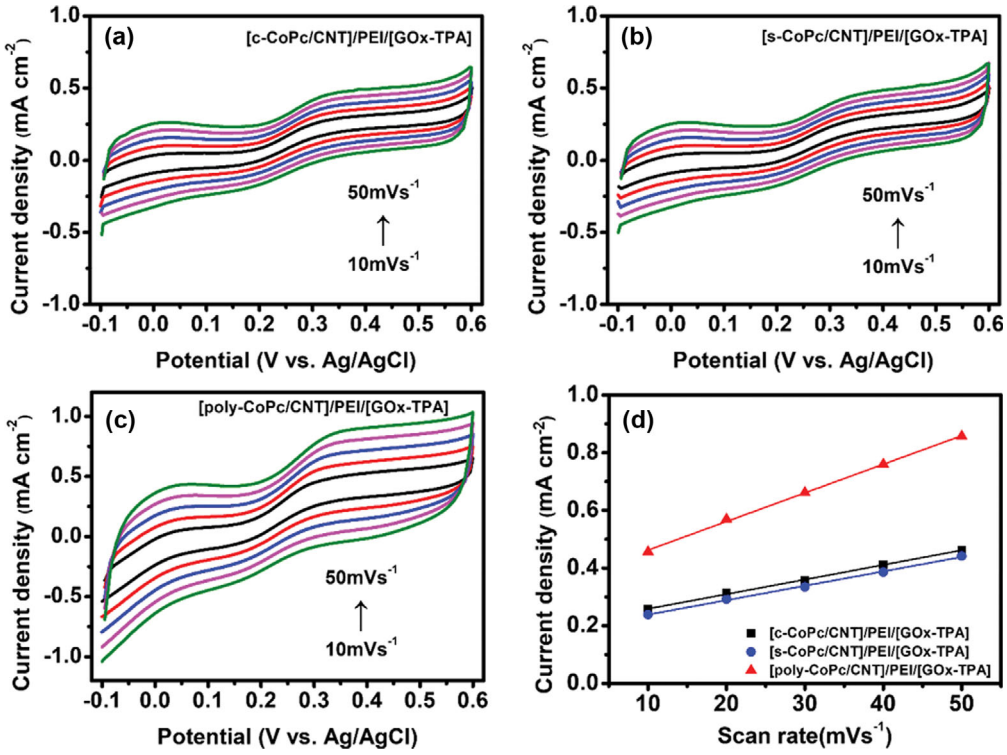

Fig. S3. CV curves of (a) [c-CoPc/CNT]/PEI/[GOx-TPA], (b) [s-CoPc/CNT]/PEI/[GOx-TPA], (c) [poly-CoPc/CNT]/PEI/[GOx-TPA] and (d) their linear regression results based on the current densities measured at 0.35 V at different scan rates (10-50 mV s^{-1}). For the tests, 10 mM glucose in 0.1 M PBS (pH 7.4) was used as the electrolyte in air saturated condition.

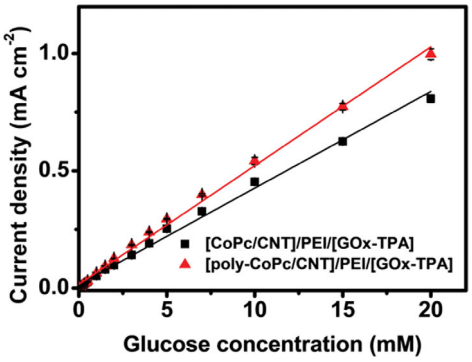

Fig. S4. Chronoamperometric response Linear regression results based on the current densities measured at 0.45 V when 0, 0.1, 0.2, 0.3, 0.4, 0.5, 1, 1.5, 2, 3, 4, 5, 7, 10, 15 and 20 mM of glucose were injected. For the tests, 0.1 M PBS (pH 7.4) was used as the electrolyte in air saturated condition, and the potential scan rate was 20 mV s^{-1}.

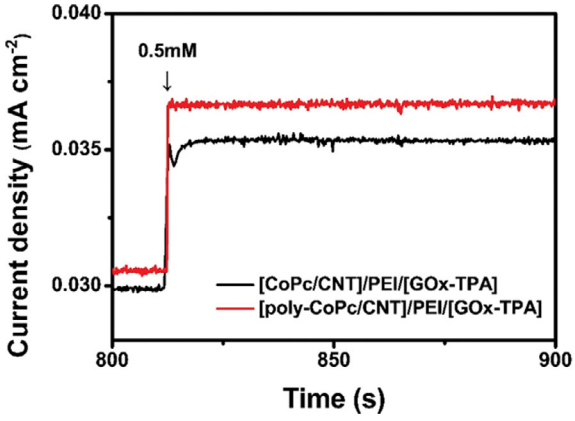

Fig. S5. Chronoamperometric response when 0.4 mM to 0.5 mM of glucose concentration changed. For the tests, 0.1 M PBS (pH 7.4) was used as the electrolyte in air-saturated condition, and responses measured at 0.45 V.

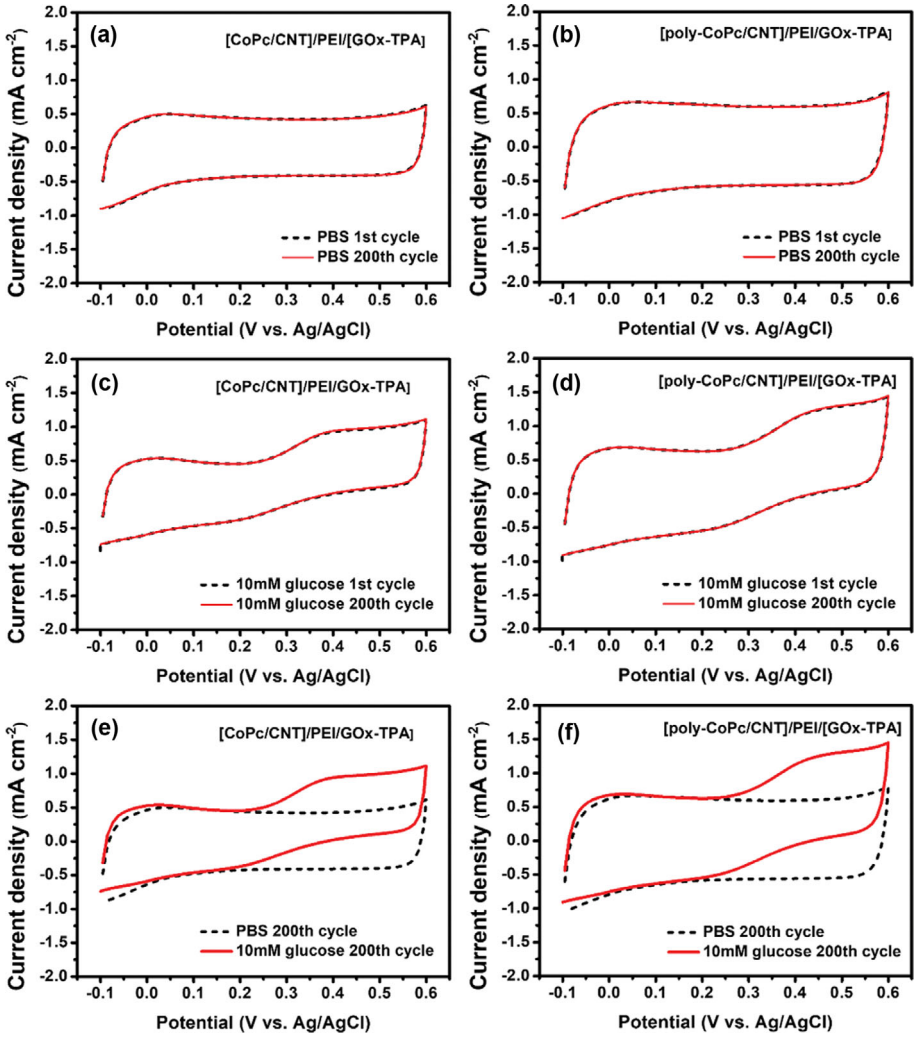

Fig. S6. CV curves of (a) [CoPc/CNT]/PEI/[GOx-TPA] and (b) [poly-CoPc/CNT]/PEI/[GOx-TPA] result when 1st cycle and 200th cycle at 0.1 M PBS (pH 7.4). (c) [CoPc/CNT]/PEI/[GOx-TPA] and (d) [poly-CoPc/CNT]/PEI/[GOx-TPA] result when 1st cycle and 200th cycle at 10 mM of glucose injected. (e) [CoPc/CNT]/PEI/[GOx-TPA] and (f) [poly-CoPc/CNT]/PEI/[GOx-TPA] result when 200th cycle for PBS condition and 10 mM of glucose injected. For the tests, 0.1 M PBS (pH 7.4) was used as the electrolyte in air saturated condition, and the potential scan rate was 100 mV s^{-1}.